Extending knowledge on the nucleophilicity of the {Pt₂S₂} core: Ph₂PCH₂CH₂PPh₂ as an alternative terminal ligand in [L₂Pt(μ-S)₂PtL₂] metalloligands †

Mercè Capdevila,[a] Yolanda Carrasco,[a] William Clegg,[b] Robert A. Coxall,[b] Pilar González-Duarte,*[a] Agustí Lledós[a] and José Antonio Ramírez[c]

[a] *Departament de Química, Universitat Autònoma de Barcelona, 08193 Bellaterra, Barcelona, Spain. E-mail: Pilar.Gonzalez.Duarte@uab.es*
[b] *Department of Chemistry, University of Newcastle, Newcastle upon Tyne, UK NE1 7RU*
[c] *Departament de Química Inorgànica, Facultat de Química, Universitat de València, Dr. Moliner 50, 46100 Burjassot, València, Spain*

The reaction of $[Pt_2(dppe)_2(\mu\text{-}S)_2]$ **1**, with metal complexes or metal salts gave different types of complexes depending on the nature of the heterometal and of the stoichiometric ratios employed. Thus, a trinuclear complex of formula $[Pt(dppe)\{Pt_2(dppe)_2(\mu_3\text{-}S)_2\}]Cl_2$ **2** and an apparently mixed Pd_xPt_{3-x} product **3** have been prepared and characterised. Alternatively, dissolution of **1** in chlorinated solvents affords **2** easily and **3** is formed from **1** with $[PdCl_2(dppe)]$. The pentanuclear complexes of formula $[M\{Pt_2(dppe)_2(\mu_3\text{-}S)_2\}_2]X_2$ (M = Zn **4** or Cd **5**, X = ClO_4; M = Cd, X_2 = $[CdCl_4]$ **5′**; M = Hg, X_2 = $[PF_6][HgCl_4]_{0.5}$ **6**) have been obtained. The structures of complexes **2**, **3**, **4**, **5**, **5′** and **6** have been determined crystallographically. Complex **2** comprises three slightly distorted square-planar *cis*-PtP₂S₂ co-ordination planes sharing two μ₃-S ligands. X-Ray data and NMR studies in solution of different crops of crystals support that **3** is essentially a simple solid-solution mixture of pure complexes $[Pd(dppe)\{Pt_2(dppe)_2(\mu_3\text{-}S)_2\}][BPh_4]_2$ **3′** and $[Pt(dppe)\{Pd_2(dppe)_2(\mu_3\text{-}S)_2\}][BPh_4]_2$ **3″** in variable proportions with at most a minor component of the homometallic complex **2**. The structure of the cations of complexes **4**, **5**, **5′** and **6** comprises two {Pt₂S₂} butterflies linked through sulfur to the metal(II) ion, which shows a significantly distorted tetrahedral environment. All complexes have been fully characterised by multinuclear NMR techniques and the corresponding parameters are reported.
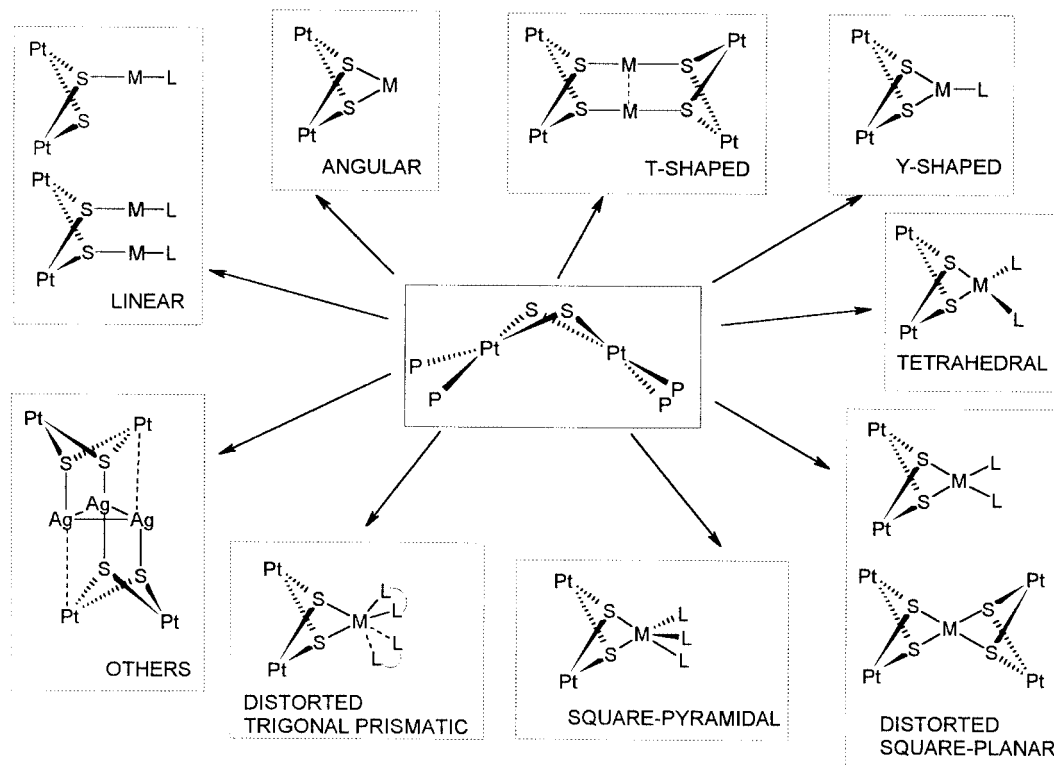
Introduction

The significant number of known homo- and hetero-metallic derivatives of $[L_2Pt(\mu\text{-}S)_2PtL_2]$, L = phosphine, shows that this species is one of the most effective metalloligands identified to date. This can mainly be attributed to the geometric features of the central Pt₂S₂ ring with a flexible hinge angle between the two $Pt^{II}S_2$ planes, and to the ability of the bridging sulfide ligands to co-ordinate additional metal ions. At the same time the wide range of co-ordination environments offered by main group or transition metals together with the nature of their accompanying species, either ligands or counter ions, enhances the structural diversity of this family of derivatives. An extensive and rigorous account on the synthesis, structures and reactivities of aggregates containing the {M₂S₂} core (M = Pd or Pt) has recently been provided by Fong and Hor.[1] Derivatives of $[L_2Pt(\mu\text{-}S)_2PtL_2]$ of known structure are summarised in Scheme 1, which includes varied co-ordination geometries about the heterometal: linear,[2] angular,[3] T-shaped,[4] Y-shaped,[5] tetrahedral,[6] square-planar,[7] square-pyramidal,[5c,6b] distorted trigonal prismatic[8] and others,[9] and displays the ability of the $[L_2Pt(\mu\text{-}S)_2PtL_2]$ metalloligand to function as a unidentate,[2] bridging,[4,9] or chelating ligand.[3,5–8]

Despite the high number of derivatives based on the Pt(μ-S)₂-Pt core,[2–10] the synthetic routes reported for complexes of formula $[L_2Pt(\mu\text{-}S)_2PtL_2]$ are not straightforward,[1] often leading to mixtures of products, and reports on their crystal

structures are scarce. We note that synthesis of most of the sulfide-bridged aggregates with the {M₂S₂} core has been achieved using monodentate phosphines, especially PPh₃, as a terminal ligand in the $[L_2M(\mu\text{-}S)_2ML_2]$ unit. Our group showed the possibilities offered by the use of bidentate phosphines. Indeed, we recently obtained significant yields of pure $[Pt_2(dppe)_2(\mu\text{-}S)_2]$ by monitoring the reaction by means of ³¹P NMR and determined its structure.[11] This showed that the central Pt₂S₂ ring is hinged in agreement with our previous theoretical *ab initio* studies for the $[Pt_2(PH_3)_4(\mu\text{-}S)_2]$ complex.[12] In addition, the preparation of $[Pt_2(dppe)_2(\mu\text{-}S)_2]$ allowed the synthesis and structure determination of pentanuclear $[Cu\{Pt_2(dppe)_2(\mu_3\text{-}S)_2\}_2]^{2+}$, which constituted the first example of an homoleptic copper(II) sulfide complex.[11] No example structurally characterised by X-ray diffraction where the heterometal is tetrahedrally co-ordinated to two $[L_2Pt(\mu\text{-}S)_2PtL_2]$ molecules had previously been reported.

In this work we report on the synthesis and characterisation of homo- and hetero-nuclear complexes derived from $[Pt_2(dppe)_2(\mu\text{-}S)_2]$ **1**. The crystalline nature of the trinuclear complex $[Pt(dppe)\{Pt_2(dppe)_2(\mu\text{-}S)_2\}]Cl_2$ **2** (*i.e.* $[Pt_3(dppe)_3(\mu_3\text{-}S)_2]$-Cl₂) and the pentanuclear complexes $[M\{Pt_2(dppe)_2(\mu\text{-}S)_2\}_2]X_2$ (M = Zn **4** or Cd **5**, X = ClO_4; M = Cd, X_2 = $[CdCl_4]$ **5′**; M = Hg, X_2 = $[PF_6][HgCl_4]_{0.5}$ **6**) has enabled us to determine their molecular structures, which are preserved in solution according to multinuclear ³¹P-{¹H}, ¹⁹⁵Pt-{¹H}, ¹¹³Cd-{¹H}, ¹¹¹Cd-{¹H} and ¹⁹⁹Hg-{¹H} NMR data. The reaction of **1** with $[PdCl_2(dppe)]$ afforded apparently a series of complexes of formula $[Pd_xPt_{3-x}(dppe)_3(\mu_3\text{-}S)_2][BPh_4]_2$ **3**, the values of *x* being determined by the solubility of pure $[Pd(dppe)\{Pt_2(dppe)_2-(\mu_3\text{-}S)_2\}][BPh_4]_2$ **3′** and $[Pt(dppe)\{Pd_2(dppe)_2(\mu_3\text{-}S)_2\}][BPh_4]_2$ **3″** and the concentration of the reactants. Single-crystal diffraction

LINEAR   ANGULAR   T-SHAPED   Y-SHAPED   TETRAHEDRAL   OTHERS   DISTORTED TRIGONAL PRISMATIC   SQUARE-PYRAMIDAL   DISTORTED SQUARE-PLANAR

Scheme 1

studies together with analytical and ^{31}P-$\{^{1}H\}$ and ^{195}Pt-$\{^{1}H\}$ NMR data indicate that the cation of **3** is essentially a mixture of those in **2**, **3′** and **3″**.

Experimental

General remarks

Metal complexes of formula [MCl₂(dppe)] were prepared according to published methods, M = Pd[13] or Pt,[14] with minor modifications. The synthesis of complex **1** has been described.[11] In the following preparations conventionally dried and degassed solvents were used and the manipulations were carried out under an atmosphere of pure dry nitrogen. **CAUTION**: perchlorate salts of metal complexes with organic ligands are potentially explosive.

Microanalyses were performed with a Carlo-Erba NA-1500 analyser. Infrared spectra in the range 4000–400 cm⁻¹ were recorded from KBr discs on a Perkin-Elmer 1710 spectrophotometer, all NMR spectra in (CD₃)₂SO solution at room temperature (^{31}P-$\{^{1}H\}$, ^{195}Pt-$\{^{1}H\}$, ^{113}Cd-$\{^{1}H\}$ and ^{111}Cd-$\{^{1}H\}$ at 121.4, 64.2, 66.5 and 63.6 MHz) on a Varian UNITY300 spectrometer. Some ^{31}P-$\{^{1}H\}$ NMR spectra have been recorded at 101.2 MHz on a Bruker AM 250 MHz, and some ^{195}Pt-$\{^{1}H\}$ and ^{199}Hg-$\{^{1}H\}$ on a Bruker AM-400 spectrometer at 85.6 and 71.6 MHz, respectively. The best ^{113}Cd-$\{^{1}H\}$ and ^{111}Cd-$\{^{1}H\}$ NMR spectra were obtained at 44.4 and 42.4 MHz, respectively, on a Bruker AM 200 MHz spectrometer. The ^{113}Cd and ^{111}Cd nuclei, $I = 1/2$, have similar abundance and neither is especially difficult to observe; ^{113}Cd is somewhat less abundant (12.26%) but has *ca.* 10% more sensitivity, and ^{111}Cd (12.75%) has a resonance frequency very close to that of ^{195}Pt, so that both can be measured simultaneously without readjusting the spectrometer probe. The ^{31}P and ^{195}Pt chemical shifts are relative to external 85% H₃PO₄ and 0.1 mol dm⁻³ Na₂PtCl₆, respectively, ^{113}Cd and ^{111}Cd to external 0.1 mol dm⁻³ Cd(NO₃)₂ aqueous solutions [δ(Cd(NO₃)₂) = δ(Cd(ClO₄)₂) − 12.7] and ^{199}Hg to 1 mol dm⁻³ HgI₂ as reference but the values given are referenced to HgMe₂ [δ(HgMe₂) = δ(HgI₂) − 3106].[15] The NMR spectra were simulated on a Pentium-200 computer using

the gNMR V4.0.1 program[16] which allows iteration from the experimental spectra, considers all isotopomers and works very well for species containing at most twelve NMR active nuclei.

Preparations

[Pt₃(dppe)₃(μ₃-S)₂]Cl₂ 2. To a solution of complex **1** (0.100 g, 0.08 mmol) in acetone (75 ml) solid [PtCl₂(dppe)] (0.053 g, 0.08 mmol) was added with stirring. After 24 h the yellow solution was concentrated to dryness affording the expected product (Found: C, 38.20; H, 3.00; S, 2.45. Calc. for C₇₈H₇₂Cl₂P₆Pt₃S₂·6CHCl₃: C, 38.35; H, 3.00; S, 2.45%). Alternatively, complex **2** was obtained by slow evaporation of a solution of **1** in CHCl₃ at room temperature. This second method yielded yellow crystals, which were suitable for X-ray analysis.

[PdₓPt₃₋ₓ(dppe)₃(μ₃-S)₂][BPh₄]₂ 3. To a solution of complex **1** (0.110 g, 0.09 mmol) in acetonitrile (50 ml) was added [PdCl₂(dppe)] (0.050 g, 0.09 mmol). After 24 h of stirring the mixture became an almost clear solution. The stoichiometrically required amount of sodium tetraphenylborate (0.060 g, 0.18 mmol) was then added. The white solid formed, NaCl, was filtered off and the filtrate allowed to stand at 4 °C for 12 h. At this stage several crops of crystals were subsequently separated from the mother solution. Analytical data for the different crops showed that the value of *x* in the formula of this material was variable. A single crystal resulting from a middle crop was chosen for X-ray diffraction.

[Zn{Pt₂(dppe)₂(μ₃-S)₂}₂][ClO₄]₂ 4. A solution of Zn(ClO₄)₂ (0.027 g, 0.10 mmol) in 15 ml methanol was added to a solution of complex **1** (0.220, 0.18 mmol) in the same solvent (100 ml). After 30 min of stirring the resultant pale yellow solution was concentrated. Addition of diethyl ether resulted in the appearance of a white solid that was filtered off, washed with cold methanol and dried. Yield 60% (Found: C, 43.55; H, 3.60; S, 4.70. Calc. for C₁₀₄H₉₆Cl₂O₈P₈Pt₄S₄Zn: C, 45.15; H, 3.60; S, 4.65%). Recrystallisation of **4** in methanol gave rise to yellow crystals adequate for X-ray diffraction. Alternatively, the same cationic [Zn{Pt₂(dppe)₂(μ₃-S)₂}₂]²⁺ species with [ZnCl₄]²⁻
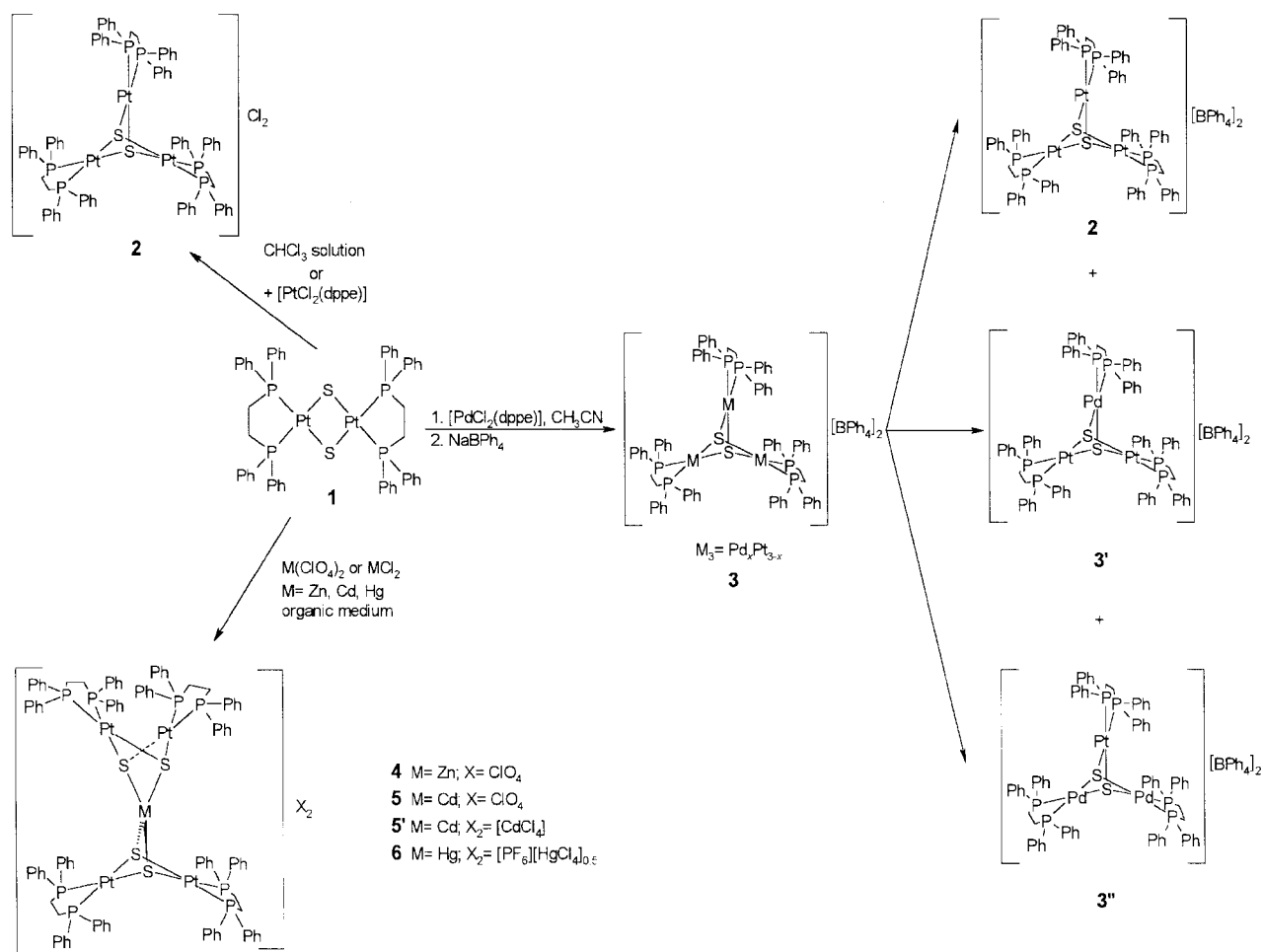
Scheme 2

instead of ClO_4^- counter ions was obtained by treating **1** with $ZnCl_2$ in the same solvent at an 1:1 stoichiometric ratio.

[Cd{Pt$_2$(dppe)$_2$(μ_3-S)$_2$}$_2$][ClO$_4$]$_2$ 5. By the same procedure as that indicated for complex **4**, a white solid separated from a methanolic solution (100 ml) containing Cd(ClO$_4$)$_2$·6H$_2$O (0.034 g, 0.08 mmol) and **1** (0.195 g, 0.16 mmol). Yield 85% (Found: C, 43.70; H, 3.45; S, 4.35. Calc. for C$_{104}$H$_{96}$CdCl$_2$O$_8$-P$_8$Pt$_4$S$_4$: C, 44.40; H, 3.45; S, 4.55%). Recrystallisation of **5** in acetone allowed isolation of colourless X-ray quality crystals.

[Cd{Pt$_2$(dppe)$_2$(μ_3-S)$_2$}$_2$][CdCl$_4$] 5′. By an analogous procedure, the reaction of CdCl$_2$·2½H$_2$O (0.046 g, 0.20 mmol) and complex **1** (0.250 g, 0.20 mmol) in methanol (100 ml) afforded a white solid. Yield: 75% (Found: C, 41.50; H, 3.50; S, 4.40. Calc. for C$_{52}$H$_{48}$CdCl$_2$P$_4$Pt$_2$S$_2$: C, 43.50; H, 3.35; S, 4.45%). Recrystallization of **5′** in acetone afforded colourless single crystals.

[Hg{Pt$_2$(dppe)$_2$(μ_3-S)$_2$}$_2$][PF$_6$][HgCl$_4$]$_{0.5}$ 6. Solid HgCl$_2$ (0.016 g, 0.06 mmol) was added to a solution of complex **1** (0.150 g, 0.11 mmol) in chloroform (50 ml) and the suspension stirred for 1 h. The salt KPF$_6$ (0.022 g, 0.11 mmol) was then added to the resultant yellow solution and the reaction mixture slowly evaporated in air and room temperature. After several days a microcrystalline orange solid was collected (Found: C, 39.95; H, 3.00; S, 3.80. Calc. for C$_{104}$H$_{96}$Cl$_2$F$_6$Hg$_{1.5}$P$_9$Pt$_4$S$_4$: C, 41.30; H, 3.20; S, 4.20%). Recrystallisation of **6** from acetone gave orange crystals suitable for X-ray diffraction.

X-Ray crystallography

Crystals of complexes **2**, **3**, **5**, **5′** and **6** were examined on Bruker AXS SMART CCD diffractometers. The small crystal size and weak X-ray scattering of complex **4** made synchrotron data collection necessary; a conventional Mo-Kα X-ray source was used for the other complexes. Methods were as described previously.[17,18] Semi-empirical absorption corrections were applied. The structures were solved by direct methods, and were refined on F^2 values for all unique reflections. Disorder in phenyl rings and anions was modelled with the aid of restraints on geometry and displacement parameters. The disorder of Pt and Pd atoms on common sites in the structure of compound **3** was freely refined subject only to a total of one metal atom on each of the three sites; no overall Pt:Pd ratio was assumed. The largest residual electron density features (ranging from just over 1 e Å^{-3} in compounds **1** and **2** to 4 e Å^{-3} in **6**) were close to metal atoms and disordered groups. Programs were standard manufacturers' control and data processing software, together with SHELXTL[19] and local programs. Crystal data are listed in Table 6, together with other information on the data collection and structure determination.

CCDC reference number 186/1559.

See http://www.rsc.org/suppdata/dt/1999/3103/ for crystallographic files in .cif format.

Results and discussion

Synthesis of the complexes

The procedures followed in the synthesis of compounds **2** to **6** are summarised in Scheme 2. The synthesis of the precursor species, [Pt$_2$(dppe)$_2$(μ-S)$_2$] **1**, has been reported.[11] It requires careful monitoring of the reaction by ^{31}P NMR in order to achieve a pure product in a reasonable yield. This diplatinum complex **1** is soluble in common organic solvents, but rapidly converts into the triplatinum complex **2** when dissolved in

chlorinated solvents. With the palladium analogue of **1** the tendency to form the trinuclear species is significantly enhanced.[20] This could well explain why the complexes of formula [Pd$_2$L$_4$-(μ-S)$_2$], L$_4$ = 4 unidentate or 2 bidentate phosphine ligands, are poorly characterised and its chemistry virtually unknown.[21]

The crystal structure of the triplatinum complex **2** shows the presence of chloride counter ions. As this complex forms easily by dissolving **1** in CHCl$_3$ or CH$_2$Cl$_2$ the only possible source of the chloride ions is the solvent molecules. This should involve the attack of the nucleophilic sulfido bridges of **1** on the chlorinated solvents, which act as electrophiles. The high nucleophilicity of the μ-thio ligands in [Pt$_2$L$_4$(μ-S)$_2$] complexes, L$_4$ = 4 unidentate or 2 bidentate phosphine ligands, towards halogenated solvents is well estabished.[1] Thus, it has been reported that upon standing in CH$_2$Cl$_2$ complexes [Pt$_2$L$_4$(μ-S)$_2$] give rise either to [PtL$_2$(SCH$_2$Cl)$_2$], L$_2$ = dppf[22] or (PPh$_3$)$_2$,[10b] or to [PtL$_2$(S$_2$CH$_2$)], L = dppy (dppy = 2-diphenylphosphanopyridine).[23] However, on the one hand in these cases formation of the corresponding trinuclear derivatives was not described and on the other we have not identified any secondary product accompanying the trinuclear compound **2**. These data seem mutually complementary and suggest that dissolution of complexes of formula [Pt$_2$L$_4$(μ-S)$_2$] in chlorinated solvents leads to formation of the [Pt$_3$L$_6$(μ$_3$-S)$_2$] trinuclear complexes together with the products of alkylation at sulfur, *viz*. [PtL$_2$(SCH$_2$Cl)$_2$] or [PtL$_2$(S$_2$CH$_2$)]. As an example, in the case of CH$_2$Cl$_2$ it seems reasonable to propose the following sequence of reactions:
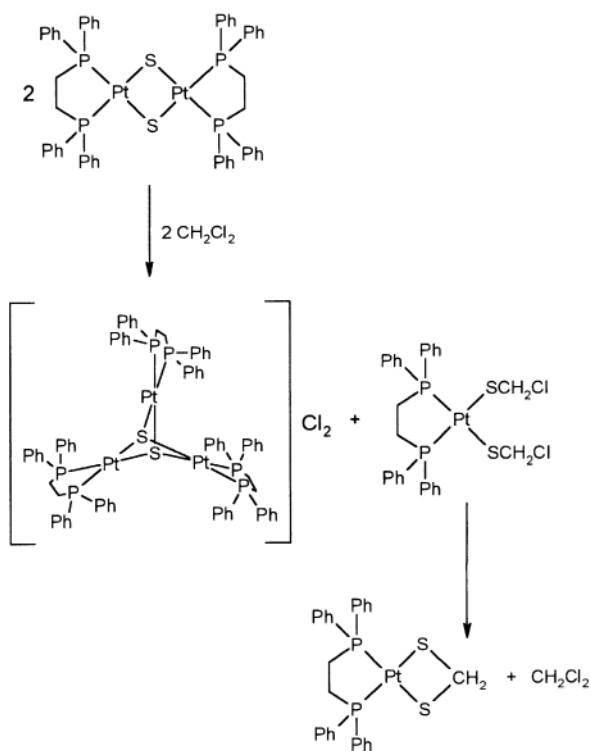
Probably, it is the solubility of each compound that determines its separation from the reaction mixture. A mechanism for the formation of various thiolato complexes from the disintegration of the {Pt$_2$S$_2$} core in CH$_2$Cl$_2$ has recently been proposed.[1] However, in this mechanism the concomitant formation of triplatinum species has not been considered. It is likely that the presence of terminal bidentate phosphines makes the nucleophilic attack of the sulfide centre on solvent molecules more difficult, thus preventing disintegration of the {Pt$_2$S$_2$} core.

Alternatively, the triplatinum complex **2** can be obtained from **1** and [PtCl$_2$(dppe)] in non-halogenated solvents. Interestingly, none of the structurally known trinuclear [M$_3$L$_6$(μ$_3$-S)$_2$] complexes, M = Ni,[24] Pd[25] or Pt,[7d,e] has been obtained from the

dinuclear [M$_2$L$_4$(μ-S)$_2$] unit. By analogy with the synthesis of the homonuclear Pt$_3$ complex **2**, it was expected that the reaction of **1** with [PdCl$_2$(dppe)] would produce the heteronuclear Pt$_2$Pd complex. However, this reaction apparently afforded a range of products of formula [Pd$_x$Pt$_{3-x}$(dppe)$_3$(μ$_3$-S)$_2$][BPh$_4$]$_2$ **3**, x being in no case exactly equal to 1 (Scheme 2). This observation can be explained on the assumption that **3** is largely a mixture of Pt$_3$ **2**, PdPt$_2$ **3′** and Pd$_2$Pt **3″**, and is in accord with the fact that these pure complexes have different solubilities in the reaction medium. Single-crystal X-ray analysis of a middle crop of crystals of **3** gives $x = 1.32$ as one of the refinement results. Moreover, ^{31}P-{^{1}H} and ^{195}Pt-{^{1}H} NMR data, discussed later, indicate that different solutions of **3** contain essentially **2**, **3′** and **3″**, those with higher content of Pt being the most soluble.

The lack of structurally known pentanuclear aggregates of formula [M{Pt$_2$L$_4$(μ-S)$_2$}$_2$]$^{2+}$ with tetrahedral co-ordination around M led us previously to the Cu^{2+} derivative.[11] To extend this family to diamagnetic metal ions, the synthesis of the analogues of Zn, Cd and Hg was undertaken. The reaction of **1** with the corresponding metal perchlorates in a 2 to 1 molar ratio led to the expected pentanuclear complexes **4** and **5**. However, the reaction of **1** with MCl$_2$ in a 1 to 1 molar ratio afforded the same [M{Pt$_2$(dppe)$_2$(μ-S)$_2$}$_2$]$^{2+}$ cations with [MCl$_4$]$^{2-}$ (M = Zn or Cd **5′**) as counter ions instead of the trinuclear [MCl$_2${Pt$_2$(dppe)$_2$(μ-S)$_2$}] species. Adducts of this formula with PPh$_3$ instead of dppe ligands for M = Zn, Cd or Hg have been obtained very recently.[26] As found in the reaction of **1** with ZnCl$_2$ and CdCl$_2$ in a 2 to 1 molar ratio, that with HgCl$_2$ led also to the pentanuclear complex **6**, but in this case the charge of two [Hg{Pt$_2$(dppe)$_2$(μ-S)$_2$}$_2$]$^{2+}$ units is compensated by one [HgCl$_4$]$^{2-}$ and two PF$_6^-$ anions. All these previous reactions occurred not only in MeOH but also in other organic solvents such as CH$_3$CN or CHCl$_3$.

Nuclear magnetic resonance data

In order to analyse the NMR data of complexes **2**–**6** it is convenient to consider those of **1** first because it is their basic structural entity. In **1**, of known structure,[11] both platinum atoms are square planar with a dihedral angle of 140° between their planes (Scheme 3). In this complex all the ^{31}P as well as all the ^{195}Pt nuclei show the same chemical shift and thus have become chemically equivalent in solution. However, neither the
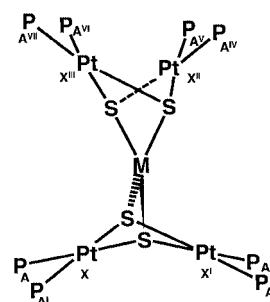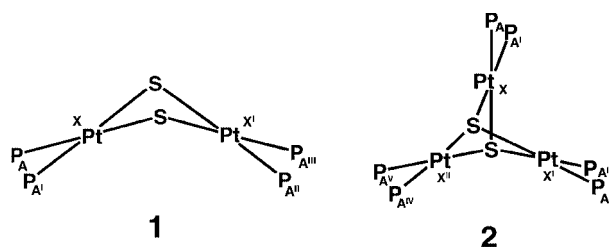
Scheme 3

Table 1 The ^{31}P and ^{195}Pt NMR parameters for complexes **1**, **2**, **3′**, **3″**, **4**, **5** and **6**

Compound		$\delta(^{195}\text{Pt})$	$\delta(^{31}\text{P})$	$^{1}J_{\text{Pt-P}}$/Hz	$^{2}J_{\text{Pt-Pt}}$/Hz	$^{3}J_{\text{Pt-P}}$/Hz	$^{4}J_{\text{P-P}}$/Hz	$^{2}J_{\text{Pt-M}}$/Hz	$^{3}J_{\text{P-M}}$/Hz
1	[Pt$_2$(dppe)$_2$S$_2$]	−4298	40.5	2740	680	−44	25		
2	[Pt$_3$(dppe)$_3$S$_2$]$^{2+}$	−4571	38.3	3248	740	−22	<10		
3′	[Pt$_2$Pd(dppe)$_3$S$_2$]$^{2+}$	−4538	40.5^a	3166	600	−23	<10		
3″	[PtPd$_2$(dppe)$_3$S$_2$]$^{2+}$	−4510	42.4^a	3131			<10		
4	[Zn{Pt$_2$(dppe)$_2$S$_2$}$_2$]$^{2+}$	−4578	37.0	3120	360	−36	10		
5	[Cd{Pt$_2$(dppe)$_2$S$_2$}$_2$]$^{2+}$	−4467	38.3	3062	180	−32	10	345^b	15^b
6	[Hg{Pt$_2$(dppe)$_2$S$_2$}$_2$]$^{2+}$	−4376	39.6	3067	200	−34	10	460	40

^{a} Refers to the phosphorus atoms bound to platinum. ^{b} Refers to ^{113}Cd coupling constants.

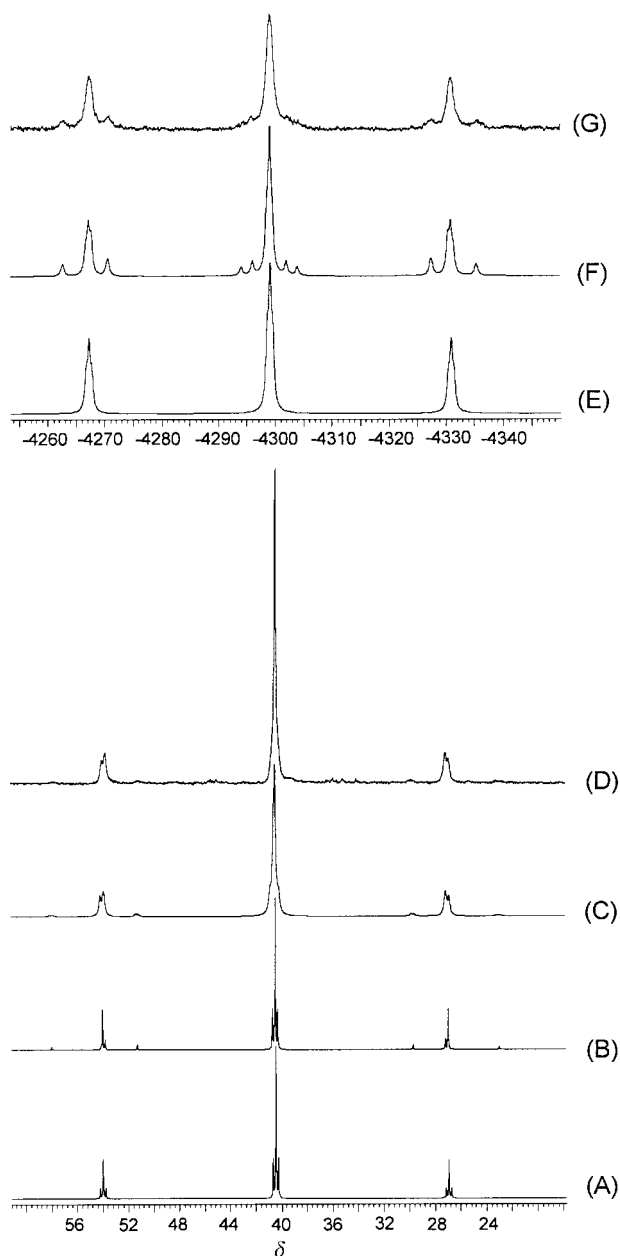**Fig. 1** The ^{31}P-{^{1}H} (bottom) and ^{195}Pt-{^{1}H} (top) NMR spectra for complex **1**, at 101.2 and 85.6 MHz, respectively: (A) ^{31}P and (E) ^{195}Pt computer simulation with no $^{2}J_{\text{Pt-Pt}}$ coupling; (B) ^{31}P and (F) ^{195}Pt computer simulation including $^{2}J_{\text{Pt-Pt}}$ coupling; (C) ^{31}P computer simulation including $^{4}J_{\text{P-P}}$ couplings; (D) ^{31}P and (G) ^{195}Pt experimental spectra.

^{31}P nor the ^{195}Pt nuclei are magnetically equivalent and thus the total spin system is (AA$^{\text{I}}$A$^{\text{II}}$A$^{\text{III}}$)XX$^{\text{I}}$.

For complex **1** the experimental ^{31}P and ^{195}Pt NMR spectra are shown in Fig. 1D and 1G, respectively. They can be interpreted with the aid of computer simulations. Initially, a first-order analysis of the ^{31}P-{^{1}H} spectrum (Fig. 1A) shows three distinct regions: downfield and upfield satellites due to $^{1}J_{\text{Pt-P}}$ and a central signal including the singlet corresponding to the phosphorus bonded to magnetically inactive platinum atoms together with sidebands due to $^{3}J_{\text{Pt-P}}$. The upfield satellite is a mirror image of the downfield, and the relative intensities of these regions agree with the relative abundance of the isotopomers (PtPt 43.8; *PtPt 44.8; *Pt*Pt 11.4%). Second order effects due to $^{2}J_{\text{Pt-Pt}}$ coupling, which is only effective for the *Pt*Pt isotopomer, give rise to new lines separated by $^{2}J_{\text{Pt-Pt}}$ in the downfield and upfield satellites (Fig. 1B). Consideration of an additional $^{4}J_{\text{P-P}}$ coupling ($^{4}J_{\text{PA-PA}^{\text{III}}} = {^{4}J_{\text{PA}^{\text{I}}\text{-PA}^{\text{II}}}}$ and $^{4}J_{\text{PA-PA}^{\text{II}}} = {^{4}J_{\text{PA}^{\text{I}}\text{-PA}^{\text{III}}}}$) leads to a general broadening of the spectral linewidth. However, for complex **1** inclusion of these long-range couplings is necessary to obtain a good fit between simulated and experimental spectra (Fig. 1C and 1D). Furthermore, the large $^{4}J_{\text{P-P}}$ value of 25 Hz found with arbitrary sign indicates a significant interaction between ^{31}P nuclei.

The ^{195}Pt-{^{1}H} spectrum of complex **1** is expected to consist basically of a triplet of triplets due to $^{1}J_{\text{Pt-P}}$ and $^{3}J_{\text{Pt-P}}$ couplings from the Pt*Pt isotopomer (Fig. 1E). Consideration of the $^{2}J_{\text{Pt-Pt}}$ coupling from the less abundant isotopomer causes the appearance of additional weak sidebands in all multiplets (Fig. 1F) and allows a good match with the experimental spectrum (Fig. 1G).

The directly deduced coupling constants together with the found chemical shift values have been used for a full computer simulation of the experimental spectra. Refinement of the parameters, including the contributions from all isotopomers leads to the final values given in Table 1.

The previous analysis of the ^{31}P and ^{195}Pt NMR data of complex **1** facilitates that of the trinuclear complexes **2**, **3′** and **3″**. Complex **2** (Scheme 3) can be described as a AA$^{\text{I}}$A$^{\text{II}}$A$^{\text{III}}$-A$^{\text{IV}}$A$^{\text{V}}$XX$^{\text{I}}$X$^{\text{II}}$ spin system, where all ^{31}P and ^{195}Pt nuclei are not magnetically equivalent but show a common chemical shift value. In this complex, the presence of three platinum atoms implies the existence of four possible isotopomers (PtPtPt 29.0; PtPt*Pt 44.4; Pt*Pt*Pt 22.7; *Pt*Pt*Pt 3.9%).

The analysis and interpretation of the experimental ^{31}P and ^{195}Pt NMR spectra of complex **2** (SUP 57611) is complicated by the second order effects appearing from virtual couplings between all three platinum nuclei and from the ^{31}P–^{31}P couplings through three or more bonds. The simulated and the experimental spectra are in good concordance. However, the linewidth does not allow a good resolution of the observed signals and thus it has only been possible to obtain partial results for the coupling constants (Table 1). In any case, the broadening of the bands suggests an upper limit of *ca.*10 Hz for $^{4}J_{\text{P-P}}$.

The ^{31}P and ^{195}Pt NMR spectra for complex **3** have allowed determination of the reaction products obtained by treatment of **1** with [PdCl$_2$(dppe)] (Scheme 2). Discussion of these results and comparison with X-ray data are given after the Molecular structures sub-section. The NMR parameters of **3′** and **3″** are given below (Table 7). Those required for comparison with the other complexes are included in Table 1.
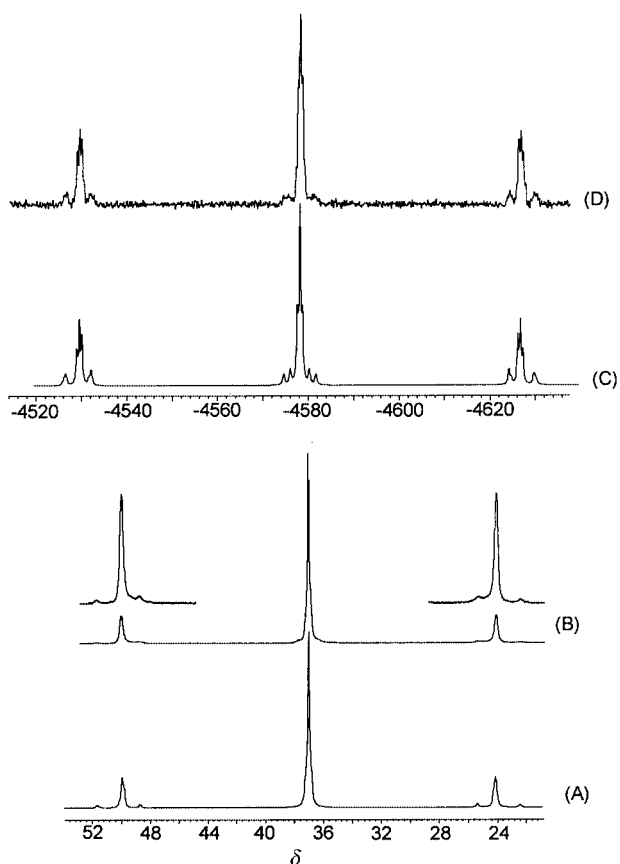
Fig. 2 The ^{31}P-$\{^1$H$\}$ (bottom) and ^{195}Pt-$\{^1$H$\}$ (top) NMR spectra for complex **4**, at 121.4 and 64.2 MHz, respectively: (A) ^{31}P and (C) ^{195}Pt computer simulations; (B) ^{31}P and (D) ^{195}Pt experimental spectra, respectively.

Comparison of the coupling constants of the trinuclear complexes **2**, **3′** and **3″** with those of the dinuclear **1** indicates that $^1J_{Pt-P}$ increases while $^3J_{Pt-P}$ and $^4J_{P-P}$ decrease. The values of $^2J_{Pt-Pt}$ are significant in both **1** and **2**, **3′**, **3″** and fall into the observed range for non-bonded metal–metal atoms.[7d,25] It is noteworthy that the structures of dinuclear and trinuclear species are strongly related, the main difference lying in the dihedral angle between platinum co-ordination planes, which is 140° in **1**[11] but reduces to 120° in **2**, **3′** and **3″** (this work).

The pentanuclear complexes (**3** in Scheme 3) should show more complicated NMR spectra as a consequence of possible interactions between the two $\{Pt_2S_2\}$ entities and of the presence of an heterometal with active isotopes in significant abundance as occurs in the cadmium (**5** and **5′**) and mercury (**6**) complexes. To analyse the relevance of the former factor, the zinc analogue **4** was synthesized and fully characterised by X-ray diffraction data (see below) and NMR in solution.

Complex **4**, whose complete spin system is AA^{I}A^{II}A^{III}-A^{IV}A^{V}A^{VI}A^{VII}XX^{I}X^{II}X^{III} (12 active nuclei), has six different isotopomers: PtPtZnPtPt 19.2; PtPtZnPt*Pt 39.4; PtPtZn*Pt*Pt 10.0; Pt*PtZnPt*Pt 20.0; Pt*PtZn*Pt*Pt 10.2 and *Pt*PtZn-*Pt*Pt 1.3%. The experimental ^{31}P-$\{^1$H$\}$ and ^{195}Pt-$\{^1$H$\}$ NMR spectra are shown in Fig. 2B and 2D, respectively. The ^{31}P-$\{^1$H$\}$ spectrum is comparable to that for complex **1** with the intense central signal due to the PtPtZnPtPt isotopomer, and with downfield and upfield signals separated by $^1J_{Pt-P} = 3120$ Hz. Although the broadening of signals makes it difficult to obtain the $^3J_{Pt-P}$ coupling values, from the separation of the weak sidebands the value of $^2J_{Pt-Pt} = 360$ Hz can be deduced. On the other hand, the ^{195}Pt-$\{^1$H$\}$ spectrum appears more resolved than that of ^{31}P-$\{^1$H$\}$ and confirms the previous coupling constants with additional information on the value of the $^3J_{Pt-P}$ coupling from the minor triplet separations. The negative sign of $^3J_{Pt-P}$ is clearly corroborated in the simulated spectrum

Table 2 Relative abundance (%) of the twelve isotopomers of the pentanuclear complexes **5**, **5′** and **6**

Isotopomer	X = Cd	X = Hg
PtPtXPtPt	14.8	16.4
PtPt*XPtPt	5.0	3.4
PtPtXPt*Pt	29.6	32.7
PtPt*XPt*Pt	9.9	6.6
PtPtX*Pt*Pt	7.4	8.2
PtPt*X*Pt*Pt	2.5	1.7
Pt*PtXPt*Pt	14.8	16.4
Pt*Pt*XPt*Pt	4.9	3.4
Pt*PtX*Pt*Pt	7.4	8.2
Pt*Pt*X*Pt*Pt	2.5	1.7
*Pt*PtX*Pt*Pt	0.9	1.0
*Pt*Pt*X*Pt*Pt	0.3	0.2
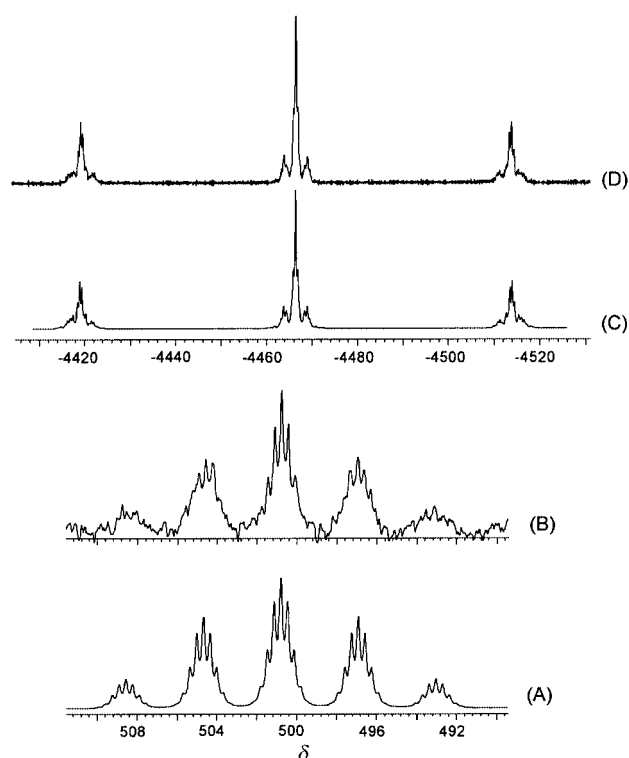
Fig. 3 The ^{113}Cd-$\{^1$H$\}$ (bottom) and ^{195}Pt-$\{^1$H$\}$ (top) NMR spectra for complex **5**, at 44.4 and 64.2 MHz, respectively: (A) simulated and (B) experimental cadmium spectra; (C) simulated and (D) experimental platinum spectra.

(Fig. 2C) by the relative intensity of the downfield and upfield satellite triplets, since only this sign combination fits well to the experimental spectrum (Fig. 2D). Both ^{31}P and ^{195}Pt NMR spectra are insensitive to the choice of sign for $^2J_{Pt-Pt}$, and a better fit occurs when a long range coupling ($^4J_{P-P} = 10$ Hz) is included.

The good match between the simulated and experimental spectra, particularly in the case of ^{195}Pt NMR (Fig. 2C and 2D), does not require consideration of additional couplings between $\{Pt_2S_2\}$ entities. Accordingly, the complete spin system (AA^{I}A^{II}A^{III}A^{IV}A^{V}A^{VI}A^{VII}XX^{I}X^{II}X^{III}Y) for the cadmium (**5**, **5′**) and mercury (**6**) analogues can be reduced to [AA^{I}A^{II}A^{III}-XX^I]$_2$Y by introducing the assumption that all couplings between nuclei of different $\{Pt_2S_2\}$ units, such as $^4J_{Pt-Pt}$, $^5J_{P-Pt}$ and $^6J_{P-P}$, are effectively zero.

Both ^{113}Cd-$\{^1$H$\}$ and ^{111}Cd-$\{^1$H$\}$ NMR spectra of complexes **5** and **5′** in solution, as a consequence of the relative abundance of different isotopomers (Table 2), should be a nonet of nonets, the first multiplet being due to coupling with the four platinum nuclei (with a $^2J_{Pt-Cd}$ separation and relative intensities 1, 16, 98, 292, 1021, 292, 98, 16, 1), and the second from long range coup-
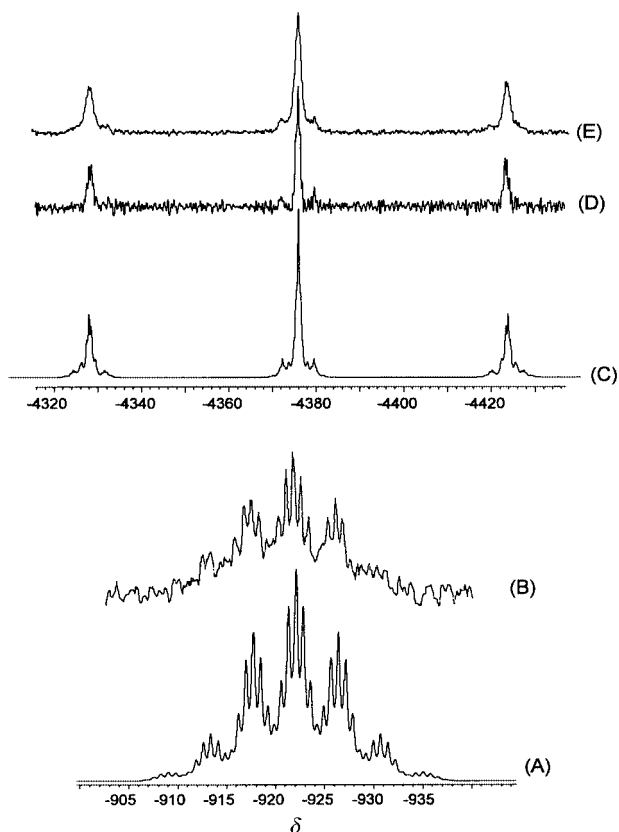
3108   *J. Chem. Soc., Dalton Trans.*, 1999, 3103–3113

Fig. 4 The ^{199}Hg-$\{^1$H$\}$ (bottom) and ^{195}Pt-$\{^1$H$\}$ (top) NMR spectra for complex 6, at 71.6 and 64.2 MHz, respectively: (A) simulated and (B) experimental mercury spectra; (C) simulated, (D) and (E) experimental platinum spectra with different resolution enhancement Fourier transform.

Fig. 5 Graphical representation of $\delta(^{31}$P$)$ vs. $\delta(^{195}$Pt$)$ chemical shifts, and $^2J_{\text{Pt-Pt}}$ vs. $^1J_{\text{Pt-P}}$ coupling constants, from Table 1, for all complexes.

ling with the eight phosphorus nuclei (with a $^3J_{\text{Cd-P}}$ separation and relative intensities 1, 8, 28, 56, 70, 56, 28, 8, 1). Disregarding the less intense bands the expected spectra should become a quintet. For both ^{113}Cd and ^{111}Cd nuclei we have observed a similar splitting of their resonance signal at about δ 501, which consists of a quintet of septets (Fig. 3B) and shows the expected relative intensities. From simulation the following coupling constants have been deduced: $^2J(^{113}$Cd-Pt$) = 345$, $^3J(^{113}$Cd-P$) = 15$, $^2J(^{111}$Cd-Pt$) = 329$ and $^3J(^{111}$Cd-P$) = 14.3$ Hz. The coupling constants involving ^{113}Cd and ^{111}Cd isotopes follow the relation $J_{113} = 1.0461 J_{111}$ in agreement with the literature.[28]

The experimental ^{199}Hg NMR spectrum for complex 6 (Fig. 4B) shows a resonance at δ -922 and consists of a multiplet similar to that observed for complexes 5 and 5′. The simulated spectrum (Fig. 4A) allows determination of the $^2J_{\text{Hg-Pt}} = 460$ and $^3J_{\text{Hg-P}} = 40$ Hz coupling values.

The ^{31}P and ^{195}Pt NMR parameters of complexes 5, 5′ and 6 given in Table 1 have been obtained through computer simulation of the experimental data. The best fit has required consideration not only of $^2J_{\text{Pt-Pt}}$ but also of $^2J_{\text{Pt-X}}$ (X = Cd or Hg). For 5 the value of $^2J_{\text{Pt-Pt}} = 180$ Hz has been deduced from the ^{31}P NMR spectrum and confirmed from the platinum spectrum, on the basis of computer simulations with different $^2J_{\text{Pt-Pt}}$ couplings. Interestingly, the $^2J_{\text{Pt-Cd}}$ ca. 340 Hz is similar to $^2J_{\text{Pt-Pt}}$ observed for complex 4. The Pt-Pt coupling has a significant effect on satellite signals of the ^{31}P NMR spectrum, while in the ^{195}Pt NMR spectrum both $^2J_{\text{Pt-Cd}}$ and $^2J_{\text{Pt-Pt}}$ couplings produce similar changes. Thus, both couplings can interfere if only first order analysis was considered.

For complex 6 the $^2J_{\text{Pt-Pt}} = 200$ Hz deduced by simulation of both ^{31}P and ^{195}Pt NMR spectra is also less than the $^2J_{\text{Pt-Hg}} = 460$ Hz. Fig. 4D and 4E show the experimental ^{195}Pt NMR spectra and Fig. 4C the simulated spectrum, which corroborates the proposed final values (Table 1). Interpretation
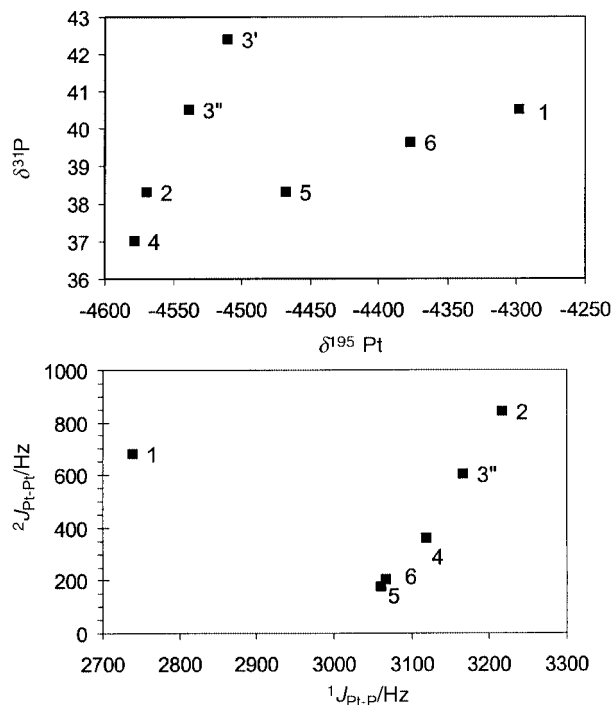
of the decrease in the Pt-Pt coupling when another significant Pt-M coupling exists is not simple because of the structural similarity among complexes 4, 5, 5′ and 6.

The previous NMR data allow us to establish interesting structure-spectroscopy correlations. The structure of the dinuclear complex 1 is known[11] and that of the trinuclear 2, 3′ and 3″ and pentanuclear complexes 4, 5, 5′ and 6 is reported in this work. A graphical representation of $\delta(^{31}$P$)$ vs. $\delta(^{195}$Pt$)$ gives two straight lines depending on the nuclearity of the complexes (Fig. 5). Thus, the pentanuclear family of complexes 4, 5, 5′ and 6 defines that with the smaller slope and includes the precursor species 1, while the trinuclear species 2, 3′ and 3″ determine a second line. Similar correlations have been reported for series of compounds and analysed through the paramagnetic term in Ramsey's equation.[29] On the other hand, another correlation between the $^2J_{\text{Pt-Pt}}$ and $^1J_{\text{Pt-P}}$ values is also observed. As shown in Fig. 5, the only species with a dihedral angle of 140° differs from the rest of the complexes, where this angle reduces to 120. Interpretation of these observations is complicated by the different factors contributing to both the chemical shifts and the coupling constants. However, experimental data on these systems may be of use in future studies on NMR data-structure relationships.

Molecular structures

Complex 2 consists of discrete trinuclear $[\text{Pt}_3(\text{dppe})_3(\mu_3\text{-S})_2]^{2+}$ cations (Fig. 6), Cl⁻ anions and chloroform solvent molecules. It is isostructural with its palladium analogue.[20] The cation has exact crystallographic C_3 symmetry with an essentially D_{3h} Pt_3S_2 core. The central unit Pt_3S_2 consists of an equilateral triangle of platinum atoms capped above and below by two sulfur atoms thus describing a regular trigonal bipyramid. These two triply bridging sulfido ligands lie equidistant, 1.532 Å above and 1.531 Å below, the Pt_3 plane. The Pt⋯Pt, S⋯S distances and the dihedral angles between P_2PtS_2 planes are shown in Table 5. Each platinum atom has square-planar coordination (Table 3), distorted by a reduction of S-Pt-S and P-Pt-P angles from ideal 90°, and by a twist of 11.2° between the PtS_2 and PtP_2 planes.

Similar structures have been observed for $\text{P}_6\text{M}_3\text{S}_2$ cores with monodentate and chelating phosphine ligands, for M = Ni,[24]

Table 3 Selected distances (Å) and angles (°) for complexes **2** and **3**

|	**2**	**3**
M · · · M	3.1185(4)	3.0690(5), 3.2159(5), 3.0878(5)
M–S	2.3634(14)	2.3529(17), 2.3687(18), 2.3434(17)
	2.3638(14)	2.3806(17), 2.3858(17), 2.3791(17)
M–P	2.2497(15)	2.2603(19), 2.2560(18), 2.2702(18)
	2.2463(15)	2.2496(18), 2.2739(18), 2.2499(18)
S–M–S	80.76(6)	80.73(6), 80.30(6), 80.95(6)
P–M–P	86.13(6)	85.19(7), 85.81(7), 85.66(7)
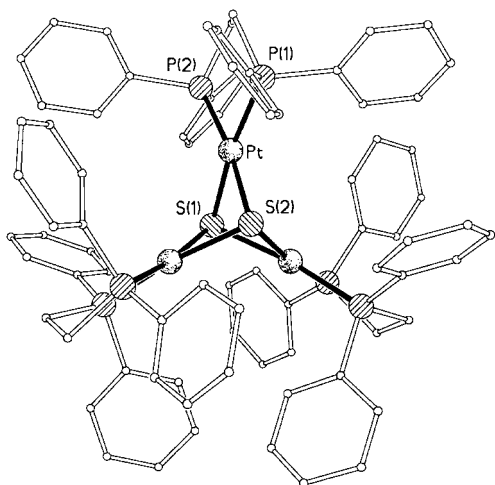
Fig. 6 The structure of the cation of complex **2**, with the labeling of independent atoms.

Pd,[25] and Pt,[7d,e] including another complex containing the same cation as **2**;[7e] none of these has crystallographic C_3 symmetry, but deviations from the ideal symmetry are not great.

Complex **3** is a mixed metal Pd/Pt analogue of **2**, but with different counter ions (BPh$_4^-$), and incorporating acetonitrile solvent in the crystal structure. The main geometrical results for the cation in **3** (Table 3) are essentially the same as those of **2** and its all-Pd analogue,[20] the two metals having the same atomic radii. In contrast, they have very different atomic scattering factors for X-rays, allowing a clear distinction between them in an ordered structure, and a relatively precise determination of the Pd : Pt occupancy ratio for each metal site in a substitutionally disordered structure. We find in the case of **3** that all three metal sites in the cation, which has no crystallographic symmetry, are disordered, but unequally so, with platinum occupancies of 59.1(4), 44.8(4), and 64.6(5)%, giving an overall formulation of Pd$_{1.32}$Pt$_{1.68}$ (56.2% Pt, 43.8% Pd) rather than PdPt$_2$ for the intended and expected trinuclear product. This empirically determined "analysis" applies only to the particular single crystal selected for X-ray diffraction study, these mixed-metal products not necessarily being homogeneous. A few heteronuclear PdPt complexes are known, in which Pd and Pt occupy chemically equivalent positions; in all cases for which crystal structures have been reported there is disorder of the metal atom sites.[26,30]

In connection with the NMR studies, it was considered particularly important to obtain a crystal structure of a Zn-centred complex such as **4**, and to demonstrate that the complex cations of Zn, Cd, and Hg had analogous structures, in order to have a reference compound with a magnetically silent heterometal. Despite repeated attempts, only very small and poorly diffracting crystals could be obtained, but these were successfully studied with synchrotron radiation facilities. Although the results are the least precise of all these structures (a reflection of the crystal quality rather than the synchrotron data collection itself), they are more than adequate for their purpose.
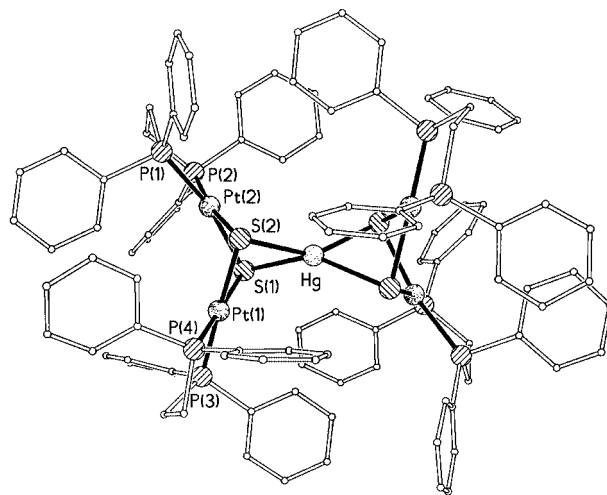
Fig. 7 Molecular structure of the cation of complex **6**, with the labeling of independent atoms.
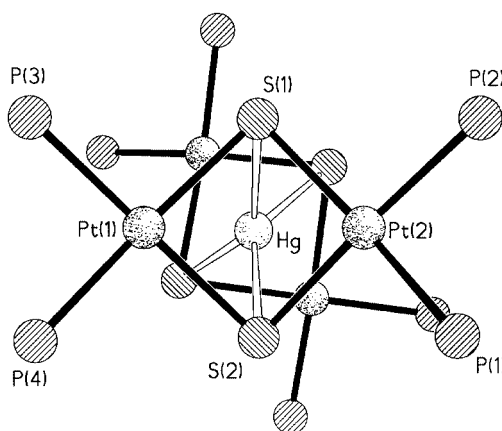
Fig. 8 Detail of the core of the cation of complex **6**.

Complexes **4**, **5**, **5′** and **6** all contain [M{[Pt(dppe)]$_2$(μ$_3$-S)$_2$}$_2$]$^{2+}$ cations (M = Zn in **4**, Cd in **5** and **5′**, Hg in **6**) together with various anions; **5′** also has solvent molecules (both acetone and water) present in the crystal structure. Complexes **4** and **5**, both with ClO$_4^-$ anions, are isostructural. The cations are all very similar (Fig. 7), consisting of two {Pt$_2$S$_2$} butterflies linked through sulfur to the heterometal, Zn, Cd or Hg, which shows a distorted tetrahedral co-ordination. They all have essentially D_2 (222) symmetry for the central core excluding C and H atoms, one of these twofold rotation axes being crystallographic for **4**, **5**, and **6**. The detailed geometry around the heterometal for **4**, **5**, **5′** and **6** is given in Table 4.

The flexibility of **1** when acting as a metalloligand can be inferred from the data collected in Table 5. In all the derivatives of **1** there is a significant reduction of the dihedral angle between PtS$_2$ planes (θ) if compared with the unbound metalloligand (140.2°). This decrease entails a concomitant shortening of the Pt · · · Pt and smaller changes in the S · · · S distances. Concerning the pentanuclear species, the high degree of distortion from the ideal tetrahedral co-ordination about the heterometal is surprising. We found a similar distortion around Cu^{II} in the complex cation [Cu{[Pt(dppe)]$_2$(μ$_3$-S)$_2$}$_2$]$^{2+}$,[11] but such a distortion is not to be expected for metals with d^{10} electronic configuration, as Zn^{II}, Cd^{II} and Hg^{II}. In all cases, the deviation from the regular tetrahedral geometry consists of a reduction of two opposite S–M–S angles (involving the chelating metalloligands) and a substantial twist of these two S–M–S planes away from the ideal 90° dihedral angle. This is shown in Fig. 8 for complex **6** as a representative example of all the pentanuclear species here reported. We do not have a ready

Table 4 Selected distances (Å) and angles (°) for complexes **4**, **5**, **5′** and **6**

	4	**5**	**5′**	**6**
M–S	2.412(6)	2.561(2)	2.579(2), 2.615(2)	2.599(2)
	2.360(6)	2.553(3)	2.555(2), 2.565(2)	2.585(2)
Pt–S	2.374(7)	2.367(2)	2.366(2), 2.374(2)	2.373(2)
	2.379(5)	2.374(2)	2.382(2), 2.379(2)	2.381(2)
	2.356(6)	2.367(2)	2.382(2), 2.376(2)	2.367(2)
	2.378(7)	2.377(3)	2.370(2), 2.371(2)	2.362(2)
Pt–P	2.243(7)	2.230(2)	2.245(2), 2.265(2)	2.242(2)
	2.262(6)	2.254(2)	2.260(2), 2.246(2)	2.246(2)
	2.268(9)	2.246(3)	2.254(2), 2.264(2)	2.259(2)
	2.274(8)	2.247(3)	2.244(2), 2.256(2)	2.242(2)
S–M–S	81.8(3), 81.4(3)	77.36(12), 76.85(10)	75.55(7), 76.39(7)	75.62(6) × 2
	114.0(2) × 2	117.14(7) × 2	113.96(7), 120.22(7)	117.57(9), 109.34(8)
	137.7(2) × 2	140.09(7) × 2	143.59(8), 139.85(8)	147.96(2) × 2
S–Pt–S	82.9(2)	84.36(8)	84.09(7), 83.66(8)	83.93(7)
	81.5(2)	84.58(10)	83.69(7), 84.03(8)	84.46(7)
P–Pt–P	85.7(3)	86.10(9)	85.15(8), 85.61(9)	86.98(8)
	85.5(3)	85.51(12)	85.45(9), 85.62(9)	86.19(8)

Table 5 Structural parameters (distances in Å, angles in °) describing the M{Pt$_2$S$_2$} core in adducts of **1**

Complex	Pt···Pt	S···S	θ^a	M···Pt	ω^b
1 [Pt$_2$(dppe)$_2$(μ-S)$_2$]^c	3.292	3.134	140.2	—	—
2 [Pt$_3$(dppe)$_3$(μ$_3$-S)$_2$]$^{2+}$	3.119	3.062	120.0	3.119	—
4 [Zn{Pt$_2$(dppe)$_2$(μ$_3$-S)$_2$}$_2$]$^{2+}$	3.083	3.144	119.8	3.129	67.0
	3.109	3.090	120.2	3.096	
5 [Cd{Pt$_2$(dppe)$_2$(μ$_3$-S)$_2$}$_2$]$^{2+}$	3.126	3.184	123.1	3.236	66.4
	3.089	3.192	126.0	3.198	
5′ [Cd{Pt$_2$(dppe)$_2$(μ$_3$-S)$_2$}$_2$]$^{2+}$	3.148	3.175	125.9	3.295; 3.160	64.1
	3.257	3.174	134.4	3.262; 3.096	
[Cu{Pt$_2$(dppe)$_2$(μ$_3$-S)$_2$}$_2$]$^{2+\,d}$	3.072	3.093	118.4	3.059; 3.057	60.0
	3.129	3.076	121.1	3.001; 3.076	
6 [Hg{Pt$_2$(dppe)$_2$(μ$_3$-S)$_2$}$_2$]$^{2+}$	3.125	3.178	125.3	3.153; 3.348	53.0

^{a} Dihedral angle between two {PtS$_2$} planes. ^{b} Dihedral angle between two {MS$_2$} planes. ^{c} Ref. 11. ^{d} Ref. 20.

Table 6 Crystallographic data for complexes **2–6**

Compound	**2**	**3**	**4**	**5**	**5′**	**6**
Formula	C$_{78}$H$_{72}$Cl$_2$P$_6$Pt$_3$S$_2$·6CHCl$_3$	C$_{126}$H$_{112}$B$_2$P$_6$Pd$_{1.32}$Pt$_{1.68}$S$_2$·MeCN	C$_{104}$H$_{96}$P$_8$Pt$_4$S$_4$ZnCl$_2$O$_8$	C$_{104}$H$_{96}$CdCl$_2$O$_8$P$_8$Pt$_4$S$_4$	C$_{104}$H$_{96}$Cd$_2$Cl$_4$P$_8$Pt$_4$S$_4$·4Me$_2$CO·2H$_2$O	C$_{104}$H$_{96}$Cl$_2$F$_6$Hg$_{1.5}$P$_9$Pt$_4$S$_4$
M	2631.7	2407.4	2766.4	2813.5	3137.1	3018.9
Crystal system	Rhombohedral	Triclinic	Orthorhombic	Orthorhombic	Triclinic	Tetragonal
Space group	$R\bar{3}c$	$P\bar{1}$	$C222_1$	$C222_1$	$P\bar{1}$	$P\bar{4}2_1c$
a/Å	18.0036(10)	14.0572(9)	13.649(8)	13.590(3)	16.7851(8)	19.4566(7)
b/Å	18.0036(10)	15.1519(9)	33.654(19)	33.847(6)	16.9057(8)	19.4566(7)
c/Å	105.495(6)	29.5450(19)	23.209(12)	22.927(4)	22.1911(10)	27.2440(10)
a/°		90.343(2)			73.093(2)	
β/°		99.877(2)			86.300(2)	
γ/°		115.552(2)			75.436(2)	
U/Å^3	29613(3)	5570.6(6)	10661(10)	10546(3)	5831.0(5)	10313.5(6)
Z	12	2	4	4	2	4
D_c/g cm^{-3}	1.771	1.435	1.724	1.772	1.787	1.944
μ/mm^{-1}	4.96	2.49	5.75	5.79	5.46	7.96
T/K	160	160	160	160	160	160
Data measured	48922	35621	24591	28842	42563	63816
$R(F)$ ('observed' data)	0.0325 (5086)	0.0624 (19221)	0.1052 (8358)	0.0485 (9640)	0.0533 (15645)	0.0359 (10766)
$R_w(F^2)$ (all data)	0.0915	0.1300	0.2295	0.1028	0.1105	0.0984
Data, parameters	5749, 411	24671, 1284	10357, 593	12427, 591	26388, 1297	12245, 603

explanation for the twist angles (ω) found but they might be related to phenyl–phenyl interactions between the two {Pt$_2$S$_2$} units. In fact, the phenyl rings from the two sides of the cation interlock quite nicely (Fig. 7), although they could probably adapt fairly easily to a different twist angle leading to greater distance between them.

The pentanuclear complexes **4**, **5**, **5′**, **6** and their copper(II) analogue are the first examples where the heterometal is tetra-hedrally co-ordinated to four sulfides from two {Pt$_2$S$_2$} units. The only other comparable complex with a M{Pt$_2$S$_2$}$_2$ core is [Pd{Pt$_2$(PPh$_3$)$_4$(μ$_3$-S)$_2$}$_2$]$^{2+}$. By contrast, it has an exactly centro-symmetric, distorted square-planar palladium(II) co-ordination in keeping with the d^8 configuration of the central metal.[7c] Similar to the palladium(II) complex, other pentanuclear arrays with four μ$_3$-S^{2-} ligands are found in [Ni{Ni$_2$Cp$_2$(μ$_3$-S)$_2$}$_2$][31] and in [Ni{Pd$_2$Cl(PPh$_3$)$_3$(μ$_3$-S)$_2$}$_2$].[32]
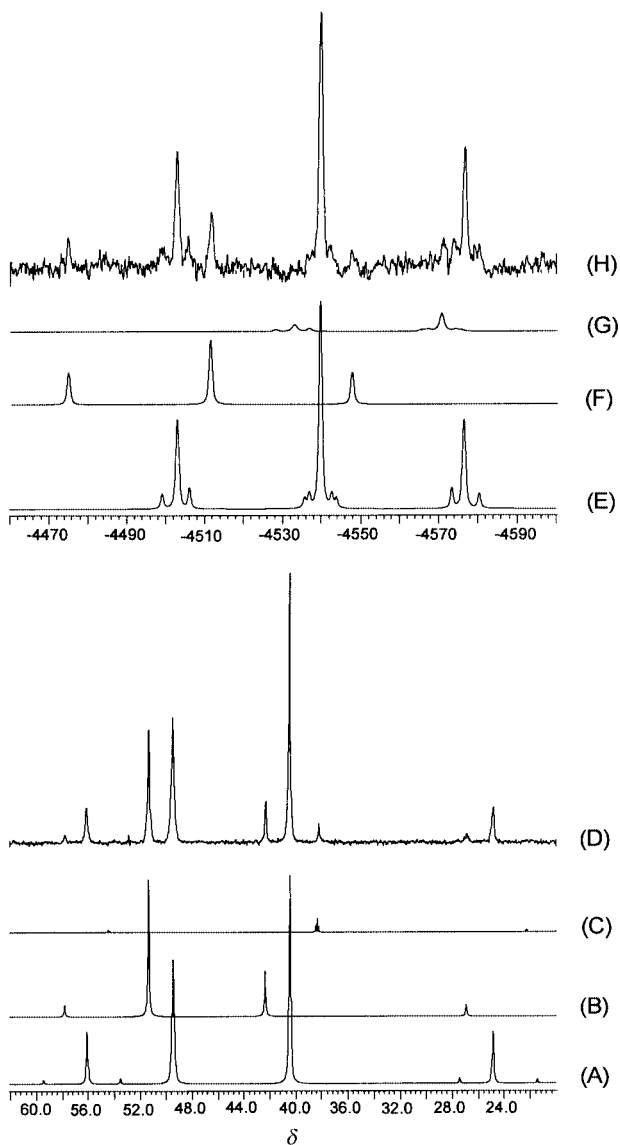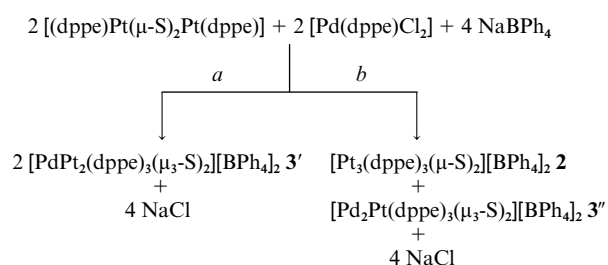
Fig. 9 The ^{31}P-$\{^1$H$\}$ (bottom) and ^{195}Pt-$\{^1$H$\}$ (top) NMR spectra for complex **3**, at 101.2 and 85.6 MHz, respectively: (A) ^{31}P and (E) ^{195}Pt computer simulation for complex **3′**; (B) ^{31}P and (F) ^{195}Pt computer simulation for **3″**; (C) ^{31}P and (G) ^{195}Pt computer simulation for **2**; (D) ^{31}P and (H) ^{195}Pt experimental spectra.

Determination of the composition of the solid solution of overall formula [Pd$_x$Pt$_{3-x}$(dppe)$_3$(μ$_3$-S)$_2$][BPh$_4$]$_2$ 3 by NMR

The different composition of the crystalline solids isolated in the reaction leading to complex **3**, which was expected to afford **3′**, finds an explanation from the analysis of the NMR spectra in solution. These data show that the reaction occurs according to two simultaneous pathways *a* and *b* (Scheme 4). Pathway *a* leads to the expected trinuclear PdPt$_2$ complex (**3′**) while *b* gives rise to two trinuclear, Pt$_3$ (**2**) and Pd$_2$Pt (**3″**), species. This second

2 [(dppe)Pt(μ-S)$_2$Pt(dppe)] + 2 [Pd(dppe)Cl$_2$] + 4 NaBPh$_4$

a   *b*

2 [PdPt$_2$(dppe)$_3$(μ$_3$-S)$_2$][BPh$_4$]$_2$ **3′**   [Pt$_3$(dppe)$_3$(μ$_3$-S)$_2$][BPh$_4$]$_2$ **2**
+   +
4 NaCl   [Pd$_2$Pt(dppe)$_3$(μ$_3$-S)$_2$][BPh$_4$]$_2$ **3″**
+
4 NaCl

Scheme 4

pathway can be explained by considering the ease of formation of **2** from **1** in solution, which allows the reaction of the remaining S$_2$Pt(dppe) fragment with [PdCl$_2$(dppe)] in a 1:2 molar ratio.

The ^{31}P-$\{^1$H$\}$ NMR spectrum of a solution of subsequent crops of the crystalline solid isolated from the reaction mixture shows formation of **3′**, but also that of **3″** and **2**. Assignment of the peaks was essentially based on NMR data for pure trinuclear **2** and its palladium analogue.[20] As observed in Fig. 9D, the experimental ^{31}P-$\{^1$H$\}$ NMR spectrum is the sum in different proportions of three individual spectra. The first one corresponds to complex **3′** and shows two different ^{31}P resonances, with relative intensity 1:2, at δ 49.5 (singlet) and at 40.5 (triplet), which can be assigned to phosphorus bound to palladium and platinum atoms, respectively (Fig. 9A). The second NMR spectrum (Fig. 9B) also displays two ^{31}P signals, at δ 51.4 (singlet corresponding to (^{31}P)$_{Pd}$) and at 42.4 (triplet assigned to (^{31}P)$_{Pt}$), with relative intensity 2:1, respectively. These features allow us to assign this spectrum to complex **3″**. Finally, the minor additional ^{31}P resonances fit very well with the presence of **2** in small proportion (Fig. 9C). The ^{31}P NMR data for **3′** and **3″** are given in Table 7. The remaining NMR parameters as well as those of **2** are included in Table 1.

The relative intensities of the three previous components in the experimental ^{31}P NMR spectrum of complex **3** (Fig. 9D) allow an estimation of the abundance of **2**, **3′** and **3″** in the crystalline product (Table 7) and thus show that **3′** is predominant in the solid mixture while **3″** and **2**, particularly the latter, form in small proportion. As, according to reaction pathway *b*, **2** and **3″** should be in a 1:1 ratio, it can be deduced that the solubility of **2** is greater than that of **3″**.

In order to corroborate the presence in solution of the unexpected heterometallic complex **3″**, the reaction of [Pd$_2$-(dppe)$_2$(μ-S)$_2$][20] and [PtCl$_2$(dppe)] was carried out. The NMR study of the samples obtained in this reaction fully agreed with data given in Table 7.

The ^{195}Pt-$\{^1$H$\}$ NMR spectrum of complex **3** (Figure 9H) confirms the coexistence of **3′**, **3″** and **2** in solution. The chemical shift values for **3′** and **3″** as well as the different coupling constants, which are in agreement with those found by ^{31}P NMR, are given in Table 1.

Based on the relative abundance of the three complexes present in solution, the overall formulation for the [Pd$_x$Pt$_{3-x}$-(dppe)$_3$(μ$_3$-S)$_2$][BPh$_4$]$_2$ complex can easily be established. The value found for *x* is very close to that calculated from the Pd:Pt occupation ratio found for each metal site by X-ray diffraction. The good concordance between NMR and X-ray data suggests that **3** is basically a solid-solution mixture of heterotrinuclear complexes. To our knowledge, this constitutes one of the few examples where it has been possible to establish the exact nature of polynuclear heterometallic PdPt complexes.[30e,j]

Conclusion

The results reported in this paper extend the knowledge on the behaviour of the [Pt$_2$(dppe)$_2$(μ-S)$_2$] metalloligand to metal ions with preference for tetrahedral co-ordination. Different counter ions and stoichiometric metalloligand to heterometal molar ratios in different solvents have always led to the pentanuclear [M$\{$Pt$_2$(dppe)$_2$(μ$_3$-S)$_2\}_2$]$^{2+}$ cations (M = Zn, Cd or Hg), which are structurally similar and show a distorted tetrahedral co-ordination around the heterometal.

In solution, the [Pt$_2$(dppe)$_2$(μ-S)$_2$] metalloligand affords the trinuclear [Pt$_3$(dppe)$_3$(μ$_3$-S)$_2$]$^{2+}$ cation easily. We propose that this expansion, Pt$_2 \longrightarrow$ Pt$_3$, is due to the nucleophilic attack of the bridging sulfur ligands on the halogenated solvents, which involves the formation of undetected sulfur alkylation products.

In the presence of [PdCl$_2$(dppe)], the [Pt$_2$(dppe)$_2$(μ-S)$_2$] metalloligand gives rise to a solid-solution mixture of the pure

Table 7 The ^{31}P NMR parameters for complexes **3′** and **3″**

Compound	$\delta(^{31}P)_{Pd}$	$\delta(^{31}P)_{Pt}$	$^1J_{Pt\text{-}P}$/Hz	Intensity ratio $(P)_{Pd}:(P)_{Pt}$	Composition (%) Solution **1**[a]	Composition (%) Solution **2**[b]
3′ [Pt$_2$Pd(dppe)$_3$S$_2$]$^{2+}$	49.5	40.5 (t)	3166	1:2	73.4	75.4
3″ [PtPd$_2$(dppe)$_3$S$_2$]$^{2+}$	51.4	42.4 (t)	3131	2:1	24.6	21.5

[a] Obtained from a first crop of crystals. The remaining percentage (2.0%) corresponds to complex **2**. These data allow calculation of the overall platinum (59.1%) and palladium (40.9%) content. [b] Obtained from a second crop of crystals. The remaining percentage (3.2%) corresponds to complex **2**. These data allow calculation of the overall platinum (60.5%) and palladium (39.4%) content.

trinuclear complexes [PdPt$_2$(dppe)$_3$(μ_3-S)$_2$]$^{2+}$, [PtPd$_2$(dppe)$_3$(μ_3-S)$_2$]$^{2+}$ and [Pt$_3$(dppe)$_3$(μ_3-S)$_2$]$^{2+}$. All three complexes have been extensively characterised by NMR spectroscopy, unambiguously confirming the genuine heteronuclear nature of the mixed-metal cations. The composition of the solid as deduced from NMR is in accordance with that calculated from X-ray diffraction data.

The pentanuclear cations have also been fully characterised by ^{31}P, ^{195}Pt, ^{111}Cd, ^{113}Cd and ^{199}Hg NMR and interesting NMR–structure correlations including the penta- and the trinuclear complexes have been found.

Acknowledgements

References

1 S.-W. A. Fong and T. S. A. Hor, *J. Chem. Soc., Dalton Trans.*, 1999, 639.

2 W. Bos, J. J. Bour, P. P. J. Schlebos, P. Hageman, W. P. Bosman, J. M. M. Smits, J. A. C van Wietmarschen and P. T. Beurskens, *Inorg. Chim. Acta*, 1986, **119**, 141.

3 M. Zhou, Y. Xu, L.-L. Koh, A. L. Tan, P.-H. Leung and T. S. A. Hor, *Inorg. Chem.*, 1993, **32**, 1875; M. Zhou, Y. Xu, A.-M. Tan, P.-H. Leung, K. F. Mok, L.-L. Koh and T. S. A. Hor, *Inorg. Chem.*, 1995, **34**, 6425.

4 C. E. Briant, T. S. A. Hor, N. D. Howells and D. M. P. Mingos, *J. Organomet. Chem.*, 1983, **256**, C15.

5 H. Liu, A. L. Tan, Y. Xu, K. F. Mok and T. S. A. Hor, *Polyhedron*, 1997, **16**, 377.

6 (*a*) H. Liu, A. L. Tan, K. F. Mok and T. S. A. Hor, *J. Chem. Soc., Dalton Trans.*, 1996, 4023; (*b*) M. Zhou, Y. Xu, C.-F. Lam, P.-H. Leung, L.-L. Koh, K. F. Mok and T. S. A. Hor, *Inorg. Chem.*, 1994, **33**, 1572; (*c*) M. S. Zhou, A. L. Tan, Y. Xu, C.-F. Lam, P.-H. Leung, K. F. Mok, L.-L. Koh and T. S. A. Hor, *Polyhedron*, 1997, **16**, 2381.

7 (*a*) D. I. Gilmour, M. A. Luke and D. M. P. Mingos, *J. Chem. Soc., Dalton Trans.*, 1987, 335; (*b*) C. E. Briant, D. I. Gilmour, M. A. Luke and D. M. P. Mingos, *J. Chem. Soc., Dalton Trans.*, 1985, 851; (*c*) C. E. Briant, T. S. A. Hor, N. D. Howells and D. M. P. Mingos, *J. Chem. Soc., Chem. Commun.*, 1983, 1118; (*d*) G. W. Bushnell, K. R. Dixon, R. Ono and A. Pidcock, *Can. J. Chem.*, 1984, **62**, 696; (*e*) M. J. Pilkington, A. M. Z. Slawin, D. J. Williams and J. D. Woollins, *J. Chem. Soc., Dalton. Trans.*, 1992, 2425.

8 M. Zhou, Y. Xu, C.-F. Lam, L.-L. Koh, K. F. Mok, P.-H. Leung and T. S. A. Hor, *Inorg. Chem.*, 1993, **32**, 4660.

9 V. W.-W. Yam, P. K.-Y. Yeung and K.-K. Cheung, *Angew. Chem., Int. Ed. Engl.*, 1996, **35**, 739.

10 (*a*) B. H. Aw, K. K. Looh, H. S. O. Chan, A. L. Tan and T. S. A. Hor, *J. Chem. Soc., Dalton Trans.*, 1994, 3177; (*b*) M. Zhou, P.-H. Leung, K. F. Mok and T. S. A. Hor, *Polyhedron*, 1996, **15**, 1737.

11 M. Capdevila, Y. Carrasco, W. Clegg, R. A. Coxall, P. González-Duarte, A. Lledós, J. Sola and G. Ujaque, *Chem. Commun.*, 1998, 597.

12 M. Capdevila, W. Clegg, P. González-Duarte, A. Jarid and A. Lledós, *Inorg. Chem.*, 1996, **35**, 490.

13 A. D. Westland, *J. Chem. Soc.*, 1965, 3060.

14 M. P. Brown, R. J. Puddephatt, M. Rashidi and K. R. Seddon, *J. Chem. Soc., Dalton Trans.*, 1977, 951.

15 R. K. Harris and B. E. Mann; *NMR and the Periodic Table*, Academic Press, London, 1978.

16 P. H. M. Budzelaar, gNMR V4.01, Cherwell Scientific, 1997.

17 C. Redshaw, V. C. Gibson, W. Clegg, A. J. Edwards and B. Miles, *J. Chem. Soc., Dalton Trans.*, 1997, 3343.

18 W. Clegg, M. R. J. Elsegood, S. J. Teat, C. Redshaw and V. C. Gibson, *J. Chem. Soc., Dalton Trans.*, 1998, 3037.

19 SHELXTL, Bruker AXS, Madison, WI, 1994.

20 M. Capdevila, W. Clegg, R. A. Coxall, P. González-Duarte, M. Hamidi, A. Lledós and G. Ujaque, *Inorg. Chem. Commun.*, 1998, **1**, 466.

21 G. Li, S. Li, A. L. Tan, W.-H. Yip, C. W. Mak and T. S. A. Hor, *J. Chem. Soc., Dalton Trans.*, 1996, 4315.

22 M. Zhou, C. F. Lam, K. F. Mok, P.-H. Leung and T. S. A. Hor, *J. Organomet. Chem*, 1994, **476**, C32.

23 V. W. W. Yam, P. K. Y. Yeung and K. K. Cheung, *J. Chem. Soc., Chem. Commun.*, 1995, 267.

24 K. Matsumoto, N. Saiga, S. Tanaka and S. Ooi, *J. Chem. Soc., Dalton Trans.*, 1991, 1265; C. A. Ghilardi, S. Midollini and L. Sacconi, *Inorg. Chim. Acta*, 1978, **31**, L431; C. A. Ghilardi, S. Midollini, A. Orlandini, C. Battistoni and G. Mattogno, *J. Chem. Soc., Dalton Trans.*, 1984, 939.

25 H. Werner, W. Bertleff and U. Schubert, *Inorg. Chim. Acta*, 1980, **43**, 199.

26 Ref. 27 (*b*) of ref. 1.

27 N. M. Boag, J. Browning, C. Crocker, P. L. Goggin, R. J. Goodfellow, M. Murray and J. L. Spencer, *J. Chem. Res. (S)*, 1978, 228.

28 P. S. Pregosin (Editor), *Transition Metal Nuclear Magnetic Resonance*, Elsevier, Amsterdam, 1991.

29 M. P. Guy, J. L. Coffer, J. S. Rommel and D. W. Bennett, *Inorg. Chem.*, 1988, **27**, 2942; S. F. Gheller, T. W. Hambley, J. R. Rodgers, R. T. C. Brownlee, M. J. O'Connor, M. R. Snow and A. G. Wedd, *Inorg. Chem.*, 1984, **23**, 2519; A. F. Masters, G. E. Bossard, T. A. George, R. T. C. Brownlee, M. J. O'Connor and A. G. Wedd, *Inorg. Chem.*, 1983, **22**, 908.

30 (*a*) H. C. Clark, G. Ferguson, V. K. Jain and M. Parvez, *Inorg. Chem.*, 1985, **24**, 1477; (*b*) *Inorg. Chem.*, 1986, **25**, 3808; (*c*) H. C. Clark, G. Ferguson, P. N. Kapoor and M. Parvez, *Inorg. Chem.*, 1985, **24**, 3924; (*d*) R. J. H. Clark, V. B. Croud, R. J. Wills, P. A. Bates, H. M. Dawes and M. B. Hursthouse, *Acta Crystallogr., Sect. B*, 1989, **45**, 147; (*e*) M. Capdevila, W. Clegg, P. González-Duarte, B. Harris, I. Mira, J. Sola and I. C. Taylor, *J. Chem. Soc., Dalton Trans.*, 1992, 2817; (*f*) T. Suzuki, N. Itaka, S. Kurachi, M. Kita, K. Kashiwavara, S. Ohba and J. Fujita, *Bull. Chem. Soc. Jpn.*, 1992, **65**, 1817; (*g*) H. Kurosawa, K. Hirako, S. Natsuma, S. Ogoshi, N. Kanehisa, Y. Kai, S. Sakaki and K. Takeuchi, *Organometallics*, 1996, **15**, 2089; (*h*) E. Colacio, R. Cuesta, M. Ghazi, M. A. Huertas, J. M. Moreno and A. Navarrete, *Inorg. Chem.*, 1997, **36**, 1652; (*i*) G. Reusmann, M. Grehl, W. Reckordt and B. Krebs, *Z. Anorg. Allg. Chem.*, 1994, **620**, 199; (*j*) W. Clegg, M. Capdevila, P. González-Duarte and J. Sola, *Acta Crystallogr., Sect. B*, 1996, **52**, 270.

31 H. Vahrenkamp and L. F. Dahl, *Angew. Chem.*, 1969, **81**, 152.

32 D. Fenske, H. Fleischer, H. Krautscheid, J. Magull, C. Oliver and S. Weisgerber, *Z. Naturforsch., Teil B*, 1991, **46**, 1384.

Paper 9/03899J